

Observational Constraints on the Origins of the Fundamental Plane

M. A. Pahre & S. G. Djorgovski

Palomar Observatory, Caltech, USA

Abstract: We review the concept of the Fundamental Plane (FP), and present new results on the near-infrared FP. We show that the K -band FP differs both from the optical form and the virial expectation under the assumption of constant (M/L) and homology. Systematic variations of only the stellar populations parameters (age, metallicity, IMF) cannot reproduce the slopes of the FP simultaneously at both the optical and near-infrared wavelengths. There appears to be an additional effect which could be due to a systematic departure of the velocity distributions of elliptical galaxies from a homologous family. In order to distinguish between the different possible stellar populations parameters, the FP and its projections can be observed at a range of redshifts. We describe several such evolutionary tests: in the intercept of the color-magnitude relation; in the intercept of the Kormendy surface brightness-radius correlation; and in the intercept of the FP itself. All three tests are fully consistent with the population of cluster elliptical galaxies having formed at high redshift; this contradicts large, systematic age variations as a significant contributor to the slope of the FP.

1. What is the Fundamental Plane?

The Fundamental Plane (FP) is a bivariate family of correlations of the properties of elliptical galaxies (Djorgovski & Davis 1987; Dressler *et al.* 1987). The properties that are usually correlated for the FP are the half-light radius r_e , the mean surface brightness (SB) $\langle\mu\rangle_e$ interior to that radius, and the central velocity dispersion σ_0 . Other parameters can be used in the FP, such as the substitution of a color or line index for σ_0 (de Carvalho & Djorgovski 1989), or the substitution of luminosity for radius. Some monovariate correlations also represent important properties among ellipticals, such as the distance-independent M_{g_2} - σ relation which may be a good age indicator (see Bender, this volume).

The FP can be projected onto any two axes out of the three variables. Examples of these projections are the color-magnitude relation, the Kormendy radius-SB relation (Kormendy 1977), and the Faber & Jackson (1976) relation between luminosity and velocity dispersion. The D_n - σ relation is another example, as it was constructed as a nearly edge-on projection of the FP (Dressler *et al.* 1987); its residuals should correlate slightly with SB (Gunn 1988), as was observed by Lucey, Bower, & Ellis (1991a).

The FP is usually expressed as a correlation of the observed properties of ellipticals, but the correlations of real interest are those of the underlying physical properties, such as galaxy mass, mass distribution, velocity distribution, luminosity density, and stellar populations parameters. The key to understanding the significance of the existence of a FP lies in determining how the observed correlations translate into constraints on underlying physical properties. For example, stellar populations effects can be found in the line strengths, colors, luminosity, and surface brightness terms which enter into the FP.

The FP is not necessarily a universal correlation for all environments. A systematic difference may exist between field and cluster ellipticals in both the intercept and scatter of the FP (de Carvalho & Djorgovski 1992). There may be slight differences between the slopes of the FP in the Coma and Virgo clusters (Lucey *et al.* 1991a) and between the cores and halos of several rich clusters (Djorgovski, de Carvalho, & Han 1989; Lucey *et al.* 1991a). Finally, there are also signs of systematic differences (possibly due to environment) between ellipticals in the Coma cluster and the Hydra–Centaurus supercluster (Guzman 1995). For the remainder of this paper, we will concentrate on ellipticals found in rich clusters of galaxies, as these seem to show the greatest homogeneity of their properties.

2. Constraints Placed on Ellipticals by the FP

Elliptical galaxies in the Coma cluster have the following FP in the V -band (Lucey *et al.* 1991b):

$$r_e \propto \sigma_0^{1.23} \langle \Sigma \rangle_e^{-0.82}. \quad (1)$$

If we assume both that light traces mass (i.e. all galaxies have the same mass-to-light ratio) and that elliptical galaxies form a homologous family, then application of the virial theorem predicts the FP relation to be:

$$r_e \propto \sigma_0^2 \langle \Sigma \rangle_e^{-1}. \quad (2)$$

The deviation of the observed $\langle \Sigma \rangle_e$ exponent from the virial expectation appears to be roughly independent of wavelength (compare Lucey *et al.* 1991b at V with Pahre, Djorgovski, & de Carvalho 1995 at K); it will not be discussed further here, but this deviation may partly be due to structural departures from a homology (Graham & Colless, this volume).

The deviation of the σ_0 exponent from the virial expectation could be caused by a breakdown of either of the two assumptions. A systematic variation in mass-to-light ratio along the FP could be due to variations in the stellar content (age, metallicity, or IMF) among ellipticals. The resulting dependence is then $(M/L) \propto M^\alpha$, where $\alpha \sim 0.24$ in the V -band. The value of α should also change with wavelength if it is due to stellar populations effects. Systematic variations in the amount of dark matter or its distribution could also create a variation in (M/L) along the FP.

If the σ_0 exponent is caused by systematic departures of the structure and dynamics of elliptical galaxies from a homology, then this effect should be strictly

independent of wavelength. There are reasons to suspect that structural nonhomology is present among elliptical galaxies due to variations in the shapes of the light profiles (Burkert 1993; Caon, Capaccioli, & D’Onofrio 1993; Hjorth & Madsen 1995; Graham & Colless, this volume). A direct analysis of the effects of structural nonhomology on the FP, however, suggests that it is insufficient to explain the slope for the σ_0 exponent in the V -band (Graham & Colless, this volume). Dynamical nonhomology is motivated in numerical simulations of dissipationless merging (Capelato, de Carvalho, & Carlberg 1995), but a wide-variety of analytical models have yet to be explored for this effect.

Regardless of explanation for the slopes of the FP, another constraint due to the FP is its extremely small scatter (see Renzini & Ciotti 1993). It is still unclear if the thickness of the FP has ever been resolved, or if its thickness can be entirely explained by observational errors. Line indices from high-quality spectra of nearby ellipticals (dominated by field and Virgo galaxies), when compared to the stellar populations models of Worthey (1994), suggest that there could be a complicated interplay between age and metallicity that manages to keep the FP thin (Worthey, Trager, & Faber 1996). The result of those data and model comparisons is a prediction that $(M/L)_K \propto \text{constant}$.

3. The Near-Infrared Fundamental Plane

As seen in §2, the slope of the near-infrared FP is a direct test on a number of models for the origin of the FP: the wavelength dependence of stellar populations effects (age, metallicity, or IMF, taken separately); nonhomology; and the age-metallicity correlations of Worthey *et al.* (1996). For this reason, we undertook a large, K -band, wide-field imaging survey of > 200 elliptical galaxies in 9 rich clusters and 2 loose groups. The data for this project were obtained with a IR cameras on the Palomar 60" telescope and the Las Campanas 40" and 100" telescopes. Velocity dispersion data were drawn from the literature. The data have all been taken and reduced; the analysis is currently underway, and preliminary results are described below. An analysis of 1/3 of the dataset in five clusters were presented by Pahre *et al.* (1995).

We find that the FP in the K -band is well-represented by the relation

$$r_e \propto \sigma_0^{1.66 \pm 0.09} \langle \Sigma \rangle_e^{-0.75 \pm 0.03}. \quad (3)$$

It is immediately apparent, via comparison with Eq. 1, that the near-infrared FP has a larger exponent in σ_0 than in the V -band; by comparing with Eq. 2, it is also clear that the near-infrared FP still deviates from the virial expectation at high confidence. The slope of the FP varies somewhat between clusters, but this effect is small and is being investigated. Nonetheless, common FP appears to represent all clusters quite well, as can be seen in Figure 1. We find the identical effect as in Guzman (1995) for a systematic difference between the Coma cluster and the Hydra-Centaurus supercluster in the distance-independent relationship between $(D_K - D_V)$ and σ_0 . We note that the FP we derive in the K -band is

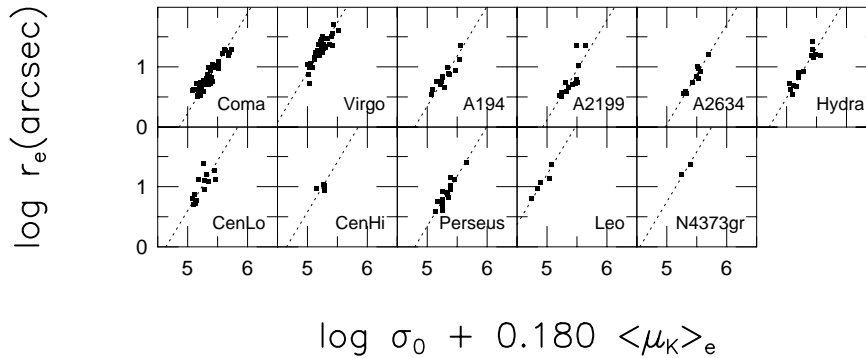


Figure 1. The near-infrared Fundamental Plane. The dotted lines displayed correspond to the least-squares fit (i.e. Eq. 3) in which the slope is fixed for all clusters, but the intercepts are allowed to vary for each cluster. A common FP appears to represent the data in all clusters well.

fully consistent with that from photoelectric photometry (Recillas-Cruz *et al.* 1990, 1991; Djorgovski & Santiago 1993).

4. An Explanation for the Slope of the FP

Now that the FP has been derived with imaging data at both optical and infrared wavelengths, it is possible to construct and test models that might explain the slope of the FP. A comparison of the expected wavelength effects of various stellar populations models (Worthey 1994), and nonhomology models, is demonstrated in Figure 2. The extent of the FP was assumed to be 4 mag in luminosity, and the ordinate is the power law in the relation $(M/L) \propto L^\beta$ (where the SB term is near unity and hence ignored). It is clear from the diagram that no stellar populations models by themselves are able to fit the slope of the FP at all wavelengths; some other effect is required which appears to be roughly independent of wavelength. Likewise, models of nonhomology alone cannot explain the data. Instead, some combination of the two effects is needed, as can be seen by the rough agreement in the right-hand panel of Figure 2.

Some of the extreme stellar populations models in Figure 2 can be excluded on the basis of other information. The extreme age model has a larger age spread (factor of 3) than even the models of Worthey *et al.* (1996; a factor of two), and the extreme metallicity model would predict a slope for the color-magnitude relation that is much steeper than observed (Bower, Lucey, & Ellis 1992). Hence, modest stellar populations effects are favored by this analysis.

It is common throughout the literature to refer to the deviation of the slope of the FP from the virial expectation as constituting an “observed dependence of mass-to-light ratio on luminosity.” As the above argument suggests, however, this might in part be due to deviations of the velocity distributions of ellipticals from a homologous family, and not due to intrinsic variations in M/L . Hence the term “observed dependence of M/L on L ” would be, at least in part, a misnomer.

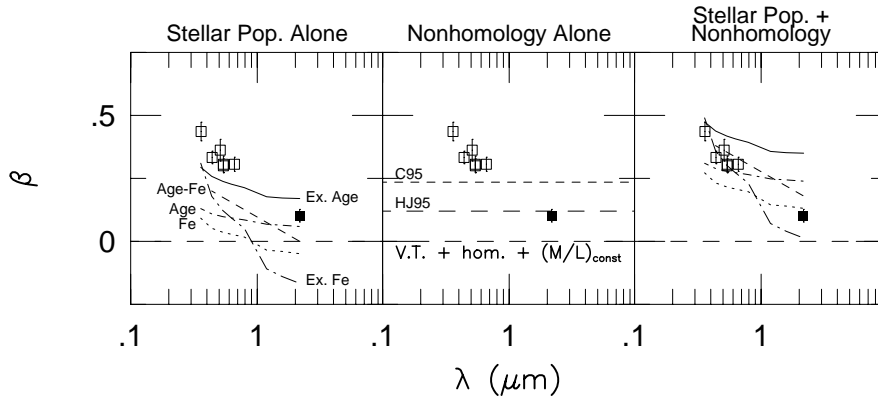


Figure 2. Fitting stellar populations models and deviations from homology to the slope of the FP at different wavelengths. The data are for cluster ellipticals at U, B, g, r from Jørgensen, Franx, & Kjaergaard (1996), V from Lucey *et al.* (1991a), and K (this paper, solid symbol). The stellar populations models [left] are labelled as follows: $-0.1 < [Fe/H] < +0.1$ (Fe); $-0.5 < [Fe/H] < +0.25$ (Ex. Fe); $9 < t < 14$ Gyr (Age); $3 < t < 9$ Gyr (Ex. Age); and the age-metallicity model of Worthey *et al.* (1996; Age-Fe). Not even the extreme models of age or metallicity can explain the slope of the FP at all wavelengths. The nonhomology models [middle] are from Capelato *et al.* (1995; C95) and Hjorth & Madsen (1995; HJ95), and also cannot explain the data. Adding the effects of nonhomology to those of the stellar populations models [left], however, allows room for significant agreement between the models and the slope of the FP at the different wavelengths.

The composite model described above makes several predictions. First, the slope of the FP should increase with increasing aperture used to measure the velocity dispersion (i.e. Capelato *et al.* 1995). While it is generally known that velocity dispersions decrease with aperture, it is not clear if this is a systematic effect, i.e. that σ decreases more rapidly with (r/r_e) for the larger ellipticals. There is such a hint in the analysis of Jørgensen *et al.* (1995) or the data of D’Onofrio *et al.* (this volume), but the scale of the observed effect may not be as dramatic as in the numerical simulations of Capelato *et al.* (1995). More work is needed to address this point. Second, if there are systematic deviations from a homology, then the stellar populations contributions to the slope of the FP are smaller than previously thought; thus there should be less evolution in the slope of the FP with redshift.

5. The FP and Its Projections at High Redshift

If there exists a significant, systematic spread in ages among the cluster elliptical galaxy population, then an excellent test of this is to observe the FP and its projections at higher redshift (see also Franx, this volume).

5.1 Color Evolution of the Early-Type Population in Clusters

The first step in observing the FP at high redshift is to define a sample of galaxies in a given cluster. We have developed a quantitative method by which to identify the cluster elliptical population in a complete, reliable, and robust way using multicolor CCD imaging data (Pahre 1996, in preparation). The key ingredient to this method is the use of a second color to discriminate low-redshift

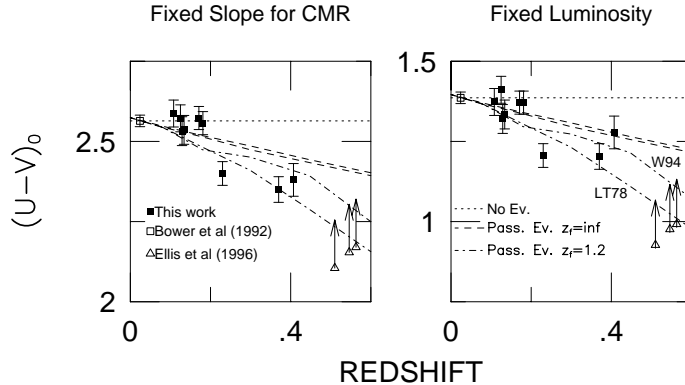


Figure 3. Color evolution in restframe $(U - V)_0$ for the early-type population in rich clusters of galaxies. A k -correction appropriate to the observed system (U, V at $z < 0.15$, B, R_C at $0.15 < z < 0.45$, and V, I_C at $z > 0.5$) has been applied to transform into the restframe U_0, V_0 . The left panel is the intercept at $V = 0$ assuming a constant slope for the CMR of -0.08 , while the right panel is a measure of the color of the CMR at a fixed luminosity of $M_V = -20.185$ ($H_0 = 75$, $\Omega_0 = 0.2$, $\Lambda_0 = 0$). There is a bluing trend with redshift for $z > 0.2$. Data at $z \sim 0.5$ from Ellis *et al.* (1996) are included, although those authors note the substantial absolute calibration uncertainty of their data (as indicated by the arrows). The models are from Worthey (1994; W94) and Larson & Tinsley (1978; LT78).

cluster ellipticals from high-redshift field spirals; this allows the individual color constraints to be applied weakly (i.e. allowing a scatter of 0.2 mag to 0.4 mag in each color). A morphological cut from the concentration index (Abraham *et al.* 1994) is also included. These selection criteria can be tested using Monte Carlo simulations to determine if the final results are biased in any way.

This method immediately produces a measurement of the color evolution of the early-type population in rich clusters using the intercept of the color-magnitude relation (CMR). By using standard filters that progressively track the restframe $(U - V)$ with redshift, the uncertainty due to k -corrections can be reduced. The results for the first nine clusters we have studied at $0.08 < z < 0.41$ are displayed in Figure 3. There is a clear bluing trend with redshift for $0.2 < z < 0.41$ which indicates a high redshift of formation for the stellar content of the cluster elliptical galaxy population as a whole. If there were a conspiracy such that at all redshifts the reddest galaxies were always, say, 3 Gyr old, then no bluing trend would be seen; this is inconsistent with the data. The small scatter of the color-magnitude relation at $z \sim 0.5$ (Ellis *et al.* 1996) could be explained by either a highly-synchronous formation of ellipticals at modest redshift, or by a less-synchronized formation at high redshift. The color evolution in Figure 3 is a separate constraint which can discriminate between these two alternatives: the latter explanation appears favored. Accurate color measurements at higher redshifts using similar selection criteria are clearly needed to strengthen and extend this result. Our results are similar to those of Rakos & Schombert (1995), although we find that the bluing trend begins at a lower redshift.

5.2 Evolution in the Kormendy Radius–Surface Brightness Relation

The Kormendy (1977) relation between SB and radius is a useful projection of the FP because it does not require the measurement of velocity dispersions. Thus it can be constructed using ground-based imaging under good seeing conditions or from HST imaging. We have done an exploratory study (Pahre, Djorgovski, & de Carvalho 1996) using Keck K -band imaging for Abell 2390 ($z = 0.23$) in $0.45''$ seeing and HST/WFPC-2 F702W data publicly available for Abell 851 ($z = 0.407$). For the latter cluster, the HST images were calibrated onto the ground-based R_C photometric system, then transformed to the K -band using colors obtained at the Palomar 60-inch telescope. The results show the power of this method in measuring the luminosity evolution (via the SB term) of the Kormendy relation for a fixed metric scale, and are displayed in Figure 4. The Tolman signal is clearly detected, as is a luminosity evolution of 0.36 ± 0.14 mag in the K -band out to $z = 0.4$. This result is fully consistent with that found by Barrientos *et al.* (1996) and Schade *et al.* (1996).

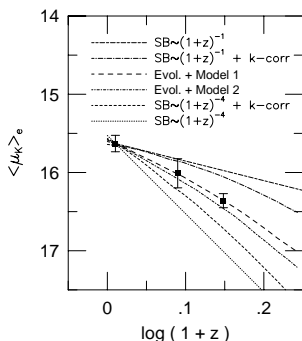


Figure 4. Evolution in the K -band Kormendy radius–SB projection of the FP, with comparison to different cosmological models (see Pahre *et al.* 1996). A correction has been applied to the tired-light models (where SB dims as $(1+z)^{-1}$) in order to account for the different metrics in the non-expanding and expanding cosmologies used for evaluating the intercept at a fixed metric size. The data are consistent with an expanding universe in which the galaxies form at high redshift and evolve passively, and are inconsistent with a non-expanding cosmology.

5.3 The FP at High Redshift Using the Keck Telescope

The most challenging step towards constructing the full FP at high redshifts is the measurement of a central velocity dispersion. Early work by Franx (1993) required long integrations (9 hours) on the MMT in order to obtain the necessary S/N on a handful of galaxies at $z = 0.18$; the Keck telescopes, on the other hand, are excellently-suited towards such observations. Displayed in Figure 5 are six sample spectra (out of 19) taken in 1.4 hours in the same $z = 0.18$ cluster which show the power of these telescopes in probing such redshifts. It is now conceivable to pursue large surveys for the FP at high redshift in modest amounts of observing time. Furthermore, small apertures can be used with the higher S/N Keck data, so that the high redshift galaxies are measured in a similar way to low redshift galaxies.

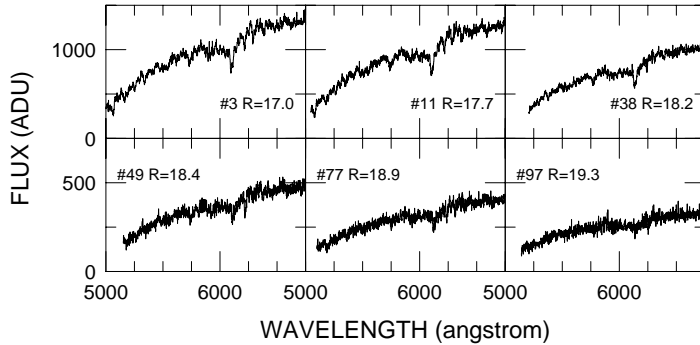


Figure 5. Sample spectra of elliptical galaxies in Abell 665 ($z = 0.18$) taken with the Keck I telescope in a 1.4 hour integration. The galaxy identifications (where the number is the ranking in that cluster among the early-type population) and the R_C -band total magnitudes are given in each panel. The apertures measured here correspond to 0.9×0.7 arcsec², which allows direct comparison with low redshift galaxies independent of assumptions on aperture corrections.

We have begun a program to measure velocity dispersions in rich clusters of galaxies at $0.08 < z < 0.75$ on the Palomar 200-inch and the Keck telescopes. Clusters at $z > 0.15$ have been chosen from those with HST/WFPC-2 optical imaging publicly available in the archive. Surface photometry in the K -band is also measured on Keck in times of good seeing (0.3 to 0.5 arcsec). The preparatory two-color CCD imaging generates the galaxy lists through the selection criteria detailed in §5.1. The first near-infrared FP at high redshift is displayed in Figure 6 for Abell 2390 ($z = 0.23$), although we note that these data are still in the preliminary reductions stages. As can also be seen from the paper by Franx (this volume), it is now clearly feasible to pursue large-scale surveys of the FP at these redshifts. Passive luminosity evolution has been detected via the change in the intercept of the FP by van Dokkum & Franx (1996).

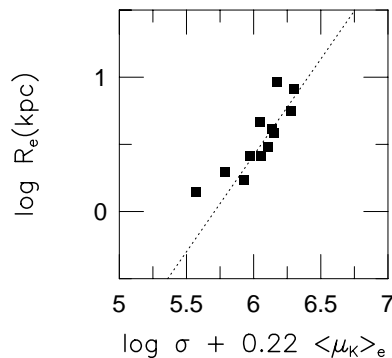


Figure 6. The near-infrared FP for Abell 2390 ($z = 0.23$) using K -band surface photometry and multiobject spectra from the Keck I 10 m telescope.

There are a number of key questions that should be addressed by these surveys of the FP at high redshift. First, how does the intercept of the FP (or the SB term at fixed radius and velocity dispersion) vary with redshift? This will allow a more accurate Tolman SB test due to the reduced scatter of the FP

itself; it will also allow the accurate measurement of the luminosity evolution of the early-type population. Second, how does the slope of the FP vary with redshift? If the slope of the FP is produced by a systematic variation in age along it, then the slope of FP should also vary with redshift. If the slope is due to metallicity variations and nonhomology, then the slope should change very little with redshift. It will be necessary to obtain a large number of galaxies per cluster (≥ 20) in order to measure the FP slope accurately. Third, how do assumptions about aperture corrections on measurements of the central velocity distribution affect the slope of the FP? Fourth, how do the slopes of the distance-independent projections of the FP vary with redshift? The Mg- σ correlation is a good age indicator (see Bender, this volume), and so it should provide a good test of the contribution of age effects to the slope of the FP. Fifth, does the slope of the FP correlate with other galaxy population parameters (like blue galaxy fraction, galaxy number density, or core profile shape or size)? And finally, what do all of these results imply for the formation history of the cluster elliptical galaxy population taken as a whole?

6. Summary

A number of different observational approaches have been described which provide constraints on possible origins for the FP. The wavelength variation of the slope of the FP has been shown to be inconsistent with all reasonable stellar populations models, requiring an additional effect such as departures of ellipticals from a homologous family. The aperture effect on velocity dispersions is a strong additional constraint on dynamical nonhomology that will need to be explored further. The evolution of the FP (Franx, this volume) and its projections (the color-magnitude and Kormendy relations) also suggest a high redshift of formation, which is in direct contradiction with possible large age spreads among ellipticals contributing to the slope of the FP. Finally, the small scatter of the FP will continue to be an additional powerful constraint for all possible origins for the slope of the FP.

MAP would like to thank the organizers for their hospitality and their invitation to present this paper. We would like to thank R. de Carvalho for many useful discussions and suggestions on a draft of this manuscript. Travel to Australia was supported by a AAS travel grant to MAP. This work was partially supported by NSF PYI award AST-9157412 to SGD, and the Bressler Foundation.

References

- Abraham, R. B., *et al.* 1994, ApJ, 432, 75
 Aragón-Salamanca, A., *et al.* 1993, MNRAS, 262, 764
 Arimoto, N., & Yoshii, Y. 1987, A&A, 173, 23
 Barrientos, L. F., Schade, D., & López-Cruz, O. 1996, ApJ, 460, L89
 Bower, R. G., Lucey, J. R., & Ellis, R. S. 1992, MNRAS, 254, 601
 Burkert, A. 1993, A&A, 278, 23

Discussion**Question: Mateo**

Which method of measuring velocity dispersions at low S/N has worked best?

Answer: Pahre

We have measured velocity dispersions with the fourier quotient, cross-correlation, and fourier fitting methods, but have not fully investigated this issue. Our preliminary reductions suggest that there is a small bias in the cross-correlation method, but not between the other two. The measurements in Figure 6 are from the fourier fitting method.

Question: Silva

Just a quick word of caution that current evolutionary population synthesis models do *not* reproduce near-IR (JHK) colors of ellipticals. So, using them to interpret the K -band FP is dangerous.

Answer: Pahre

Yes, such models do not reproduce absolute colors very well at all. Nonetheless, I have used them here solely as *differential* models—changes in colors with redshift and k -corrections—in which many of those fundamental problems are substantially lessened.

Question: Dorman

(1) Doesn't Worthey's model prediction of $(M/L)_K \propto \text{constant}$ with age arises from the notion the K -band flux is dominated by giants that don't age strongly? (2) The $(V - K)$ color involves the ratio of turnoff flux to giant flux, where K is sensitive to the latter and V is sensitive to both. Do you see $(V - K)$ evolution? (3) If $(M/L)_K \propto L^\beta$, then what sort of model can make the giant flux change like that?

Answer: Pahre

(1) Yes, I believe you are correct. (2) This is something we intend to measure in the course of our current survey; Aragón-Salamanca *et al.* (1993) found evolution in $(V - K)_0$. (3) The dependence is on the *galaxy's* luminosity L raised to the exponent β , hence there is no particular reason why the models proposed would not work. The key is what galaxy formation process could produce such a dependence of stellar populations on galaxy luminosity.

Question: Yi

Fitting the observed ($U - V$) colors as functions of redshift with (population synthesis) models should be carried out very carefully, because the model UV-U flux is “extremely” sensitive not only to age but also to several input assumptions, such as mass loss and horizontal branch mass distribution, which are often ignored in modelings.

Answer: Pahre

Certainly true. Referring to Figure 3, I have included both the Larson & Tinsley (1978) and Worthey (1994) models. As you have noted previously, the former includes no HB and hence is too blue; the latter includes only a red clump for the HB and is probably too red. The correct answer probably lies somewhere between the two.

Question: Zepf

The elemental abundance in cluster gas derived from ASCA observations require a very large number of massive stars to produce the high abundance of α elements. The mass in this massive star population is sufficiently large that the remnants from this population are a significant fraction of the observed mass in ellipticals (roughly 30%). Thus, there is a lot of room to get changes in (M/L) with L by varying the IMF with L .

Answer: Pahre

The models of Worthey (1994) do not include a galactic wind (such as in Arimoto & Yoshii 1987) hence they cannot provide any dependance of (M/L) on L as such. While your paper (Zepf & Silk 1996) makes a case that varying the IMF could produce at least part of the variation of (M/L) with L , it is still not clear if that would fully match the data in Figure 2. A wavelength-independent effect, such as nonhomology, might still be required.